ELSEVIER

Journal of Crystal Growth 186 (1998) 214–223

JOURNAL OF CRYSTAL GROWTH

AFM observation of barium nitrate {1 1 1} and {1 0 0} faces: spiral growth and two-dimensional nucleation growth

K. Maiwa*,[1], M. Plomp, W.J.P. van Enckevort, P. Bennema

RIM Laboratory of Solid State Chemistry, Faculty of Science, University of Nijmegen, Toernooiveld 1, 6525 ED Nijmegen, Netherlands

Received 5 July 1997; accepted 5 August 1997

Abstract

The growth mechanisms of the {1 1 1} and {1 0 0} faces of $Ba(NO_3)_2$ crystals growing from aqueous solutions were investigated by ex situ atomic force microscopy. Growth hillocks induced by dislocations and growth islands formed via 2D nucleation were observed on both faces. The thinnest steps observed on the {1 1 1} and {1 0 0} faces were, irrespective of step sources, $d_{1\,1\,1} = 4.7$ Å and $d_{2\,0\,0} = 4.1$ Å in height, respectively. These correspond to the elementary growth layers expected in Bravais–Friedel–Donnay–Harker (BFDH) and Hartman–Perdok (i.e. periodic bond chain) theories. The spiral hillocks on the {1 0 0} face consist of double elementary layers. On {1 1 1} faces, three kinds of spiral layers arising from single dislocations were discerned: single, double and triple elementary layers, which can be produced by dislocations with Burgers vectors $\boldsymbol{b} = \langle 1\,0\,0\rangle$, $\langle 1\,1\,0\rangle$ and $\langle 1\,1\,1\rangle$, respectively. It was observed that the multiple spiral layers tend to split into elementary steps at the spiral centres, which can be explained by entropic repulsion. It was also found that several spiral centres are accompanied with hollow cores and that the diameters of these cores vary with the number of spiral arms connected with the central dislocation. The numerous 2D nuclei of elementary height found between the spiral arms were probably created in the short period of very high supersaturation during separation of the crystal from the solution.

PACS: 81.10.Aj; 81.10.Dn; 61.16.Ch; 61.72.Fp

Keywords: Barium nitrate; Surface topography; Atomic force microscopy; Spiral growth; 2D nucleation

1. Introduction

Recently, atomic force microscopy (AFM) has been increasingly applied to the study of crystal growth by observing the growth features on crystal surfaces with a spatial resolution of nanometer scale. For crystals growing from solution, many attempts of AFM observations were done particularly on organic crystals with large molecules [1]. Only a few were done on inorganic crystals, which generally have smaller molecules/ions [2–4].

In this work, we intend to employ ex situ AFM to observe the faces of $Ba(NO_3)_2$ crystals grown in an aqueous solution. As described below, these

* Corresponding author.

[1] Present address: National Research Institute for Metals, Sengen 1-2-1, Tsukuba, Ibaraki 305, Japan.

0022-0248/98/$19.00
PII S0022-0248(97)00446-6

crystals are a good example for the study of the mechanisms of spiral growth and two-dimensional nucleation (2D) growth. From aqueous solution, $Ba(NO_3)_2$ crystals grow in shapes bounded by large $\{1\,1\,1\}$, moderate $\{1\,0\,0\}$ and small $\{2\,1\,0\}$ faces [5]. The growth features of the $\{1\,1\,1\}$ and $\{1\,0\,0\}$ faces were investigated both ex situ and in situ in large detail by the use of various observation methods [5–18]. The character of dislocations induced during growth in an aqueous solution was well studied in detail by X-ray topography [6–10] and stress birefringence microscopy [11, 12]. Combining these results and using kinetic measurements of the $\{1\,1\,1\}$ faces with the help of a Michelson interferometer, the difference in growth rates of individual spiral hillocks was found to depend on the heights of the spiral steps and consequently on the type of the dislocation at their centres [14]. Shekunov et al. showed that, using the same technique, the growth rates oscillated as a result of a change in the dominant spiral centres on both faces [10, 13]. The change from spiral growth to 2D nucleation growth as a dominant growth mechanism was also observed on the $\{1\,0\,0\}$ faces at the supersaturation $\sigma = 4.3\%$, whereas spiral growth persisted on the $\{1\,1\,1\}$ faces at the same range of σ [15].

In this paper we report the various properties and behaviour of growth layers created by different dislocation sources and 2D nucleation on both $\{1\,1\,1\}$ and $\{1\,0\,0\}$ faces of $Ba(NO_3)_2$ grown in an aqueous solution as deduced from detailed AFM observations.

2. Experimental procedure

Prior to experiments seed crystals were prepared from an aqueous solution and those with well-developed $\{1\,1\,1\}$ and $\{1\,0\,0\}$ faces were selected. The specimen crystals were subsequently grown in an unstirred aqueous solution in a thermostated growth cell of 50 ml in volume, which is provided with an optical window to make in situ observation possible [19]. The saturation temperature of the solution was 23.0°C. Crystal growth was carried out under a growth temperature higher than 21.4°C, which corresponds to supersaturations less than 4%.

Prior to AFM observation the faceted crystals were quickly removed from the growth cell and the solution remaining on crystal faces was immediately soaked-up using highly water-absorbing paper, in order to preserve the as-grown surfaces as much as possible. Crystal faces were observed both in situ and ex situ using an optical differential interference contrast microscope (DICM) to compare the surface morphology in and out of the solution. In this way the consequences of the shut-off effect can be estimated [19]. Polarized optical microscopy was applied to observe dislocations in the crystals [11, 12].

Ex situ AFM was used to study the details of the growth features on the surfaces. In AFM, a very sharp Si_3N_4 tip attached to a spring cantilever is scanned over the surface. The deflection of the cantilever, which is linear with the force between tip and sample, is measured and offered to a feedback loop, that maintains a constant force by adjustment of the tip–sample distance. Only at sudden height changes of the sample (i.e. at steps) a pulse in the deflection signal arises, because the feedback loop cannot compensate for this height difference immediately. When this deflection signal is imaged, it provides a more detailed image with more contrast, compared to the usual height image. Because of this, most of the depicted figures in this work are *force images*, made up of the deflection signal.

3. Observations

3.1. Spiral steps

3.1.1. $\{1\,1\,1\}$ faces

Two different space groups, Pa3 [20–24] and $P2_13$ [25], have been reported in X-ray and neutron diffraction studies for $Ba(NO_3)_2$ and its isomorphous crystals. From surface morphological [6, 8] and kinetic studies [13] it was deduced that no centre of symmetry occurs, so the actual space group must be $P2_13$. This result was confirmed in the present study from the surface morphology of the $\{1\,0\,0\}$ faces as will be discussed later. However, no distinct difference was detected in the surface morphology between the $\{1\,1\,1\}$ and the $\{\bar{1}\,\bar{1}\,\bar{1}\}$

faces. Therefore, in this report we shall treat both faces as having the same growth morphology.

Fig. 1 shows examples of spiral steps observed on $\{1\,1\,1\}$ faces. At least three kinds of spiral layers induced by single-dislocation outcrops were discerned: single (Fig. 1a and Fig. 1b) double (Fig. 1c) and triple spirals (Fig. 1d). Concentric loops induced by a pair of spirals with opposite signs were also found (Fig. 1b). The height of each step was determined to be 5 ± 1 Å, which can be taken as $d_{1\,1\,1}(=4.7$ Å) within the experimental error. It was noticed that for the multiple spirals the steps are

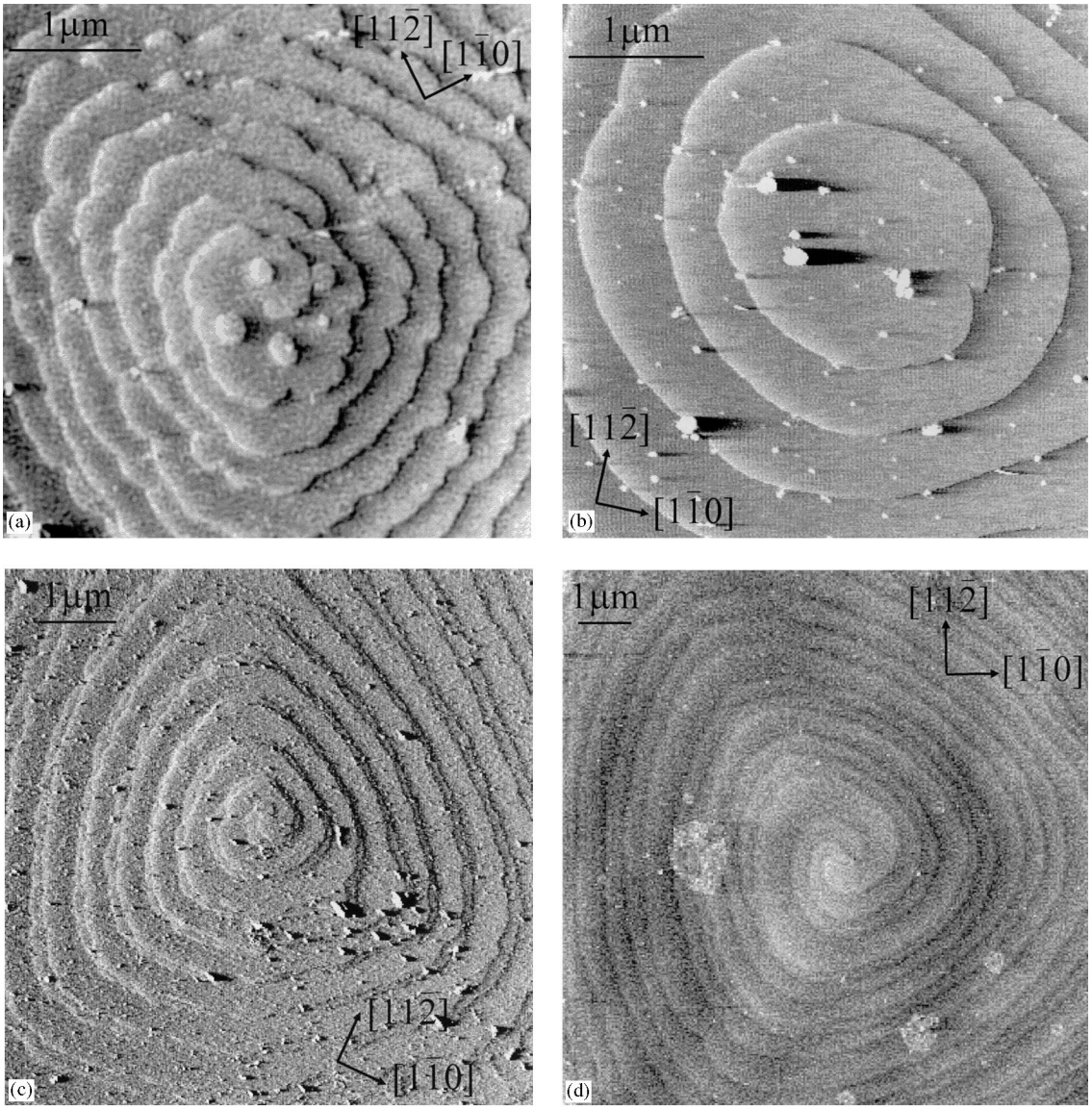

Fig. 1. Force images of spiral steps observed on $Ba(NO_3)_2$ $\{1\,1\,1\}$ faces. (a) Single spiral with a few 2D nuclei on top. (b) Concentric closed-loop steps produced by two single dislocations of opposite sign (visible on the right of the central loop). (c) Double spiral with split steps. (d) Triple spiral with split steps and 2D network on top. In all cases the step height is equivalent to $d_{1\,1\,1}$.

split into the unit-height steps $d_{1\ 1\ 1}$ directly at the spiral centres and that this step separation becomes large far from the spiral centres. From their stress birefringence images, the dislocations corresponding to the double and triple spiral steps were identified as single ones of a mixed and a screw type with Burgers vectors, $\boldsymbol{b} = [1\ 1\ 0]$ and $[1\ 1\ 1]$, respectively [11, 12]. To avoid complexity, we give here only one representative Burgers vector, e.g., $\boldsymbol{b} = [1\ 0\ 1]$ and $[0\ 1\ 1]$ are equivalent to $[1\ 1\ 0]$.

It was shown in a previous in situ observation of growth hillocks on $Ba(NO_3)_2$ $\{1\ 1\ 1\}$ faces [14], that the activities of growth centres varied depending on the types of corresponding dislocations and growth conditions. Under a high rate of solution flow, triple spirals dominated double ones and single spiral centres were not found. In contrast to the above-mentioned investigation, during the present study single spiral layers were frequently observed on the crystals, which were now grown from an unstirred solution (Fig. 1a and Fig. 1b).

Often, several dislocation outcrops located closely in an array were observed (Fig. 2a). Below these dislocations, inclusions of mother solution were correspondingly found; along the dislocation rows complex spiral centres developed (Fig. 2a). Several characteristic features of spiral growth can be noticed in Fig. 2a: (1) single, double and triple steps (denoted by s, d and t, respectively) arising from individual dislocations; (2) co-operative spiral steps originating from dislocations with the same sign (d_2, s_2 and t_3 clockwise and d_1, d_3, s_1 and s_3 anticlockwise); (3) step segments between two dislocations with opposite signs (t_1t_2, d_2d_3, d_2s_1 and d_3s_2) which will develop closed loops.

In addition to this, hollow cores were observed at the dislocations. The radii of these varied from 7 to 15 nm. It can be noted that the hollow cores that are accompanied with spiral steps increase in diameter with the number of spiral arms. Another type of hole, namely a type that does not emit steps (denoted by *e*) was also observed. Such holes retard step propagation and cause weak step bunching (Fig. 2b). Possibly these are hollow cores related to pure-edge dislocations. The detailed observation and the quantitative measurement of the hollow cores will be dealt with elsewhere [26].

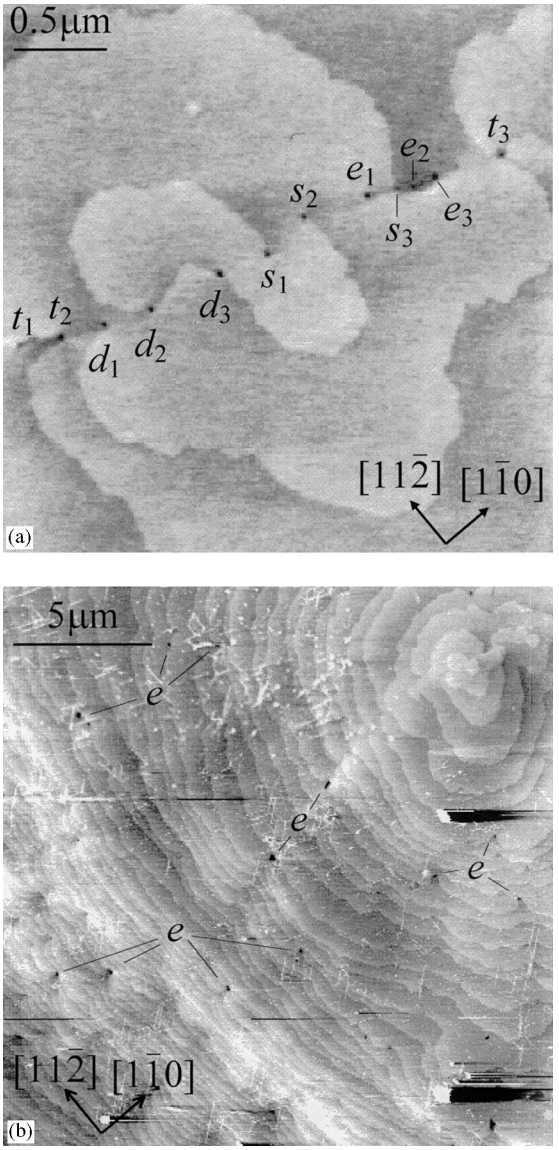

Fig. 2. Array of dislocations on a $\{1\ 1\ 1\}$ face. (a) Height image of single (*s*), double (*d*) and triple (*t*) steps in a growth hillock centre. Co-operative spiral-steps originate from clockwise (d_2, s_2 and t_3) and anti-clockwise (d_1, d_3, s_1 and s_3) dislocations, respectively; step segments between two emerging points of dislocations with opposite signs (t_1t_2, d_2d_3, d_2s_1 and d_3s_2) will develop closed patterns. (b) Lower magnification force image around the region in Fig. 2a, showing holes (*e*) that retard step propagation.

3.1.2. {1 0 0} faces

Fig. 3a shows an example of spiral hillocks observed on an (1 0 0) face. The hillock shows an ellipsoidal shape elongated in the [0 1 $\bar{2}$] direction and consists of double layers. The unit layers composing the double layers are 4 ± 1 Å in height, which is equivalent to $d_{2\,0\,0}$ (=4.1 Å) within the experimental error. It was noted that step splitting is not so pronounced as on the {1 1 1} faces. The cavities with a depth of $d_{2\,0\,0}$ on the terraces between spiral steps are characteristic for the {1 0 0} faces. Since besides the cavities also isolated 2D islands were observed on all crystals, these cavities were probably formed by the coalescence of 2D

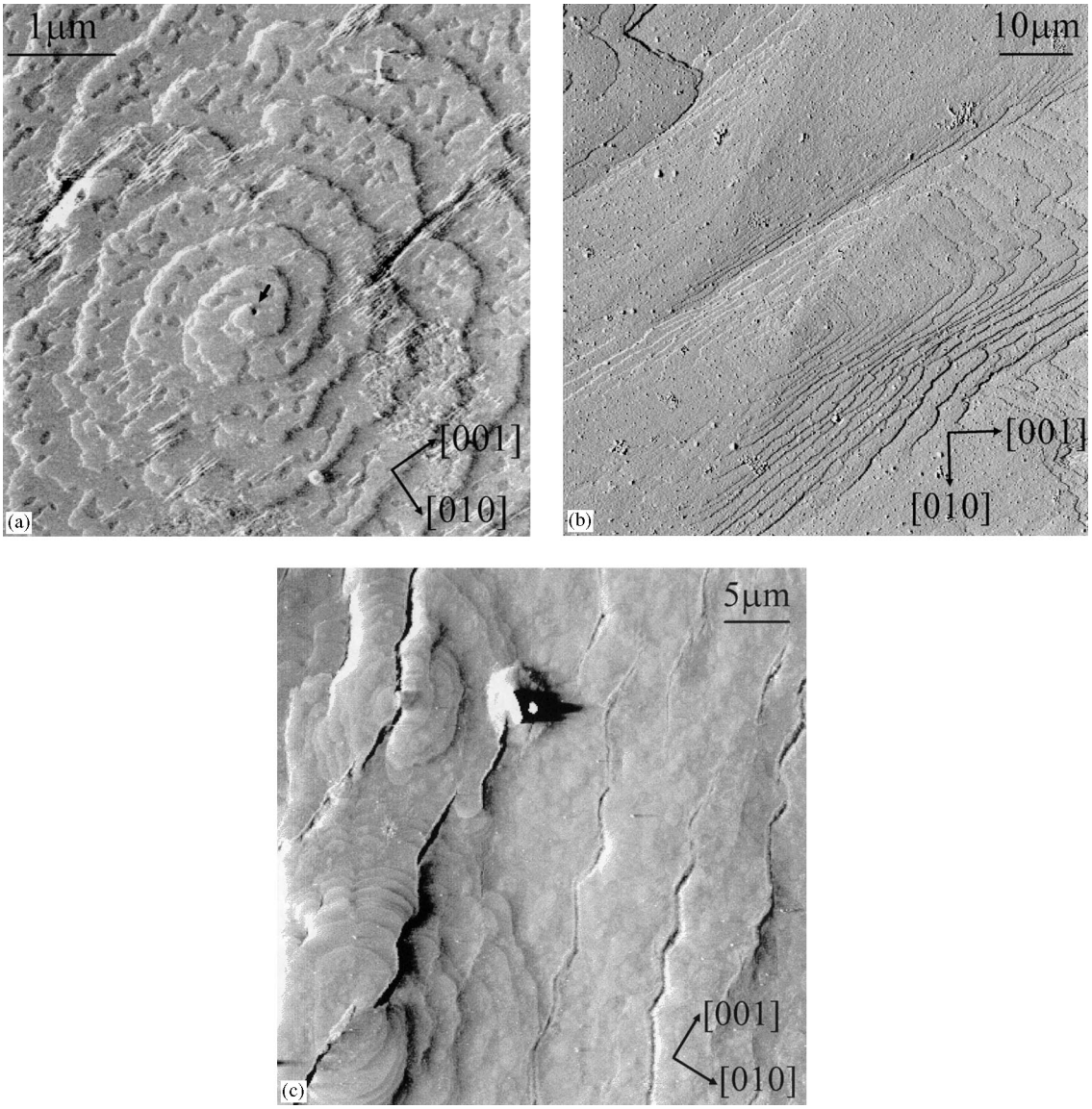

Fig. 3. Force images of growth hillocks on the $Ba(NO_3)_2$ {1 0 0} faces. (a) Double spiral with unit-height cavities in the terraces. The hollow core at the centre of the spiral is indicated by a short arrow. (b) Parallelogram-shaped hillock with bunched steps. (c) Growth hillocks intersected by 'cracks'.

nuclei formed at high supersaturation during the removal of the crystals from the solution. Hollow cores associated with spiral centres are also observed on this face (Fig. 3a). The radii of hollow cores, ranging 30–50 nm in radius, were larger than those on the {1 1 1} faces.

On the {1 0 0} faces often another type of growth hillock was observed as shown in Fig. 3b. The hillocks had parallelogram shapes of which the long sides were parallel to [0 1 $\bar{2}$] on an (1 0 0) face and, contrarily, parallel to [0 1 2] directions on an opposite ($\bar{1}$ 0 0) face. Here the indices of the faces and the crystallographic directions are assigned according to Refs. [8, 13]. The remarkable bunching of steps nearly parallel to the long sides of the hillocks is in agreement with the striations observed by Ribet and Authier [8] and is characteristic for an {1 0 0} face growing in a stagnant solution. This phenomena was clearly visible after removing the crystal from the solution. The different orientations of the growth hillocks on the opposite (1 0 0) and ($\bar{1}$ 0 0) faces indicates the absence of centrosymmetric symmetry. Therefore, the space group symmetry of $Ba(NO_3)_2$ must be $P2_13$ instead of Pa3. The spiral nature of this type of growth hillocks could not be discerned because of the strong bunching.

The polygonized and anisotropic shapes of the growth hillocks on the {1 0 0} faces of Fig. 3b are quite different from those observed during previous experiments in flowing solutions [15] and those shown in Fig. 3a. A similar change of hillock shapes on the (1 0 0) faces of $Ba(NO_3)_2$ in relation with impurity content and supersaturation of a solution was reported by Shekunov et al. [10]. They observed that the shapes of growth hillocks were nearly circular in a purer solution. On the other hand, in a solution containing some amount of impurity, the growth hillocks were rectangular at low supersaturations and became rounded upon an increase in supersaturation.

An example of the most commonly observed type of hillock is shown in Fig. 3c. The hillocks are intersected by deep 'cracks', which seem to have crystallographic directions. The two hillock sides near a crack often develop differently, which indicates that the crack was created before the hillock. Furthermore, the centres of these hillocks are very high, so that a spiral nature of these hillocks could not be discerned either. The cause of the cracks is not clear yet.

3.2. Two-dimensional nucleation

3.2.1. {1 0 0} faces

Fig. 4 shows growth islands formed by a two-dimensional (2D) nucleation mechanism on an (1 0 0) face. The isolated, small islands are elongated along approximately the [0 1 $\bar{2}$] direction, which is the direction of the long side of the parallelogram shaped growth hillocks defined in the previous section. Each growth island has the same height as a unit layer of spiral steps, namely $d_{2\,0\,0} = 4.1$ Å. In Fig. 4, at least four layers of different height level can be recognized; the birth- and spread-growth mechanism is clearly verified in this picture.

The growth islands covered the {1 0 0} faces of all crystals observed ex situ. A kinetic study of the $Ba(NO_3)_2$ (1 0 0) faces [15] showed that 2D nucleation can take place at supersaturations above $\sigma = 0.4\%$ on a surface free from dislocation outcrops. However, on crystal faces on which screw or

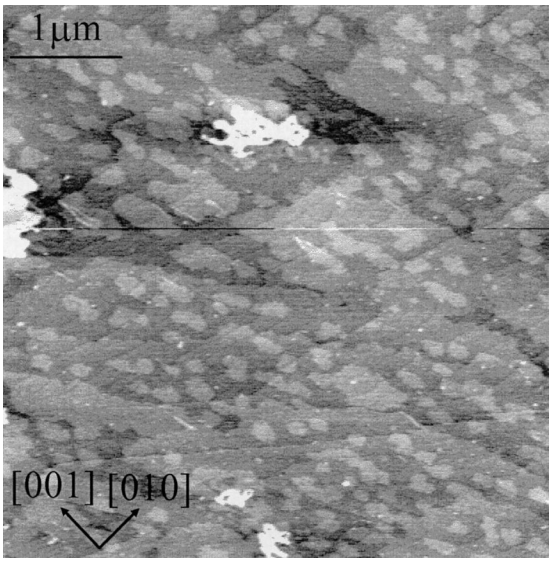

Fig. 4. Height image of 2D nucleation islands with a height of $d_{2\,0\,0} = 4.1$ Å on top of a $Ba(NO_3)_2$ (1 0 0) face. The islands are slightly elongated along the [0 1 $\bar{2}$] direction.

mixed-type dislocations emerge, the spiral growth mechanism dominates the 2D nucleation growth up to $\sigma = 5\%$. Since during the present study crystal growth was carried out at supersaturations below 4%, it can now be concluded that the 2D nuclei on the surfaces must have been formed during the period of removing the crystals from the growth cell, when $\sigma \geqslant 5\%$.

3.2.2. {1 1 1} faces

Fig. 5 shows 2D nuclei formed on an {1 1 1} face. The successive, parallel steps are spiral steps generated by a dislocation emerging somewhere else on the surface. The sharp bends of the successive steps coincide with the boundary of a droplet of solution that remained on the surface after soaking up the solution from the surface.

The height of 2D nuclei was determined to be 5 ± 1 Å, which agrees with the height $d_{1\,1\,1}$ of single spiral steps. In contrast with an {1 0 0} face, 2D nuclei on an {1 1 1} face show nearly circular shapes. It is interesting to note that 2D nuclei were only seen on the relatively large terraces between the spiral steps. This suggests that the undulated fronts of the spiral are caused by a coalescence of the spiral steps and 2D nuclei. In the previous in situ observation study of the growth of {1 1 1} faces [14], it was found that spiral growth governed the growth of these faces and 2D nucleation was not observed in the experimental range of supersaturation up to 6%. Therefore, the 2D nucleation observed on the {1 1 1} faces in this study probably occurred due to a very high supersaturation of at least 6% during separation of the crystal from the solution at the end of the growth experiment.

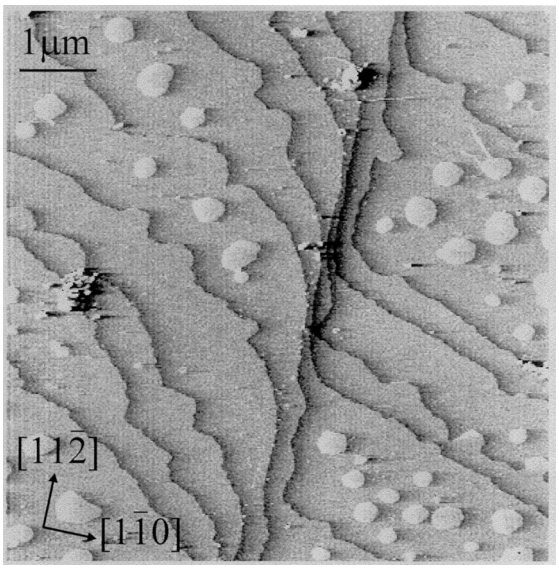

Fig. 5. Force image of 2D nuclei with a height of $d_{1\,1\,1} = 4.7$ Å on top of a $Ba(NO_3)_2$ {1 1 1} face. The successive steps originate from a dislocation elsewhere; the sharp bending of the steps at the centre of the picture corresponds to the boundary of a droplet of solution that remained on the surface after soaking up the solution from the surface.

4. Discussion

4.1. Properties and sources of steps

It was confirmed that $d_{1\,1\,1}$ and $d_{2\,0\,0}$ steps on {1 1 1} and {1 0 0} faces, respectively, were elementary steps in both 2D nucleation growth and spiral growth of $Ba(NO_3)_2$ crystals in an aqueous solution. This result agrees with the Bravais–Friedel–Donnay–Harker (BFDH) laws and the Hartman–Perdok (i.e. periodic bond chain) theory [27], which implies that the thickness of a growth layer on a crystal surface is equal to the slice thickness $d_{h\,k\,l}$ corrected for the systematic extinctions of the space group.

By the studies on lattice defects of $Ba(NO_3)_2$ crystals grown from an aqueous solution [6–10], several types of dislocations have been found. From the fact that for spiral growth the total height of steps emitted by the dislocations must be equal to the component of the dislocations' Burgers vectors $\boldsymbol{b}$ perpendicular to the crystal surface, it follows that three kinds of spiral layers are possible on (1 1 1) faces, namely (1) single spiral layers produced by the mixed-type dislocations with $\boldsymbol{b} = [1\,0\,0]$ and $[\bar{1}\,1\,1]$; (2) double spiral steps produced by the mixed-type dislocations with $\boldsymbol{b} = [1\,1\,0]$ and (3) triple spiral steps produced by the screw dislocations with $\boldsymbol{b} = [1\,1\,1]$. Pure edge dislocations with $\boldsymbol{b} = [\bar{1}\,1\,0]$ have also been reported [9] but no spiral step can be formed from such dislocations. The dislocations corresponding to the double and the triple spiral layers as well as the edge

dislocations could be identified by polarized microscopy [11, 12].

It is interesting to compare the sizes of hollow cores and the types of spiral centres in relation to the dislocation properties. It has been shown theoretically that the radii of hollow cores at dislocation outcrops depend on, amongst others, the strains of dislocations and the supersaturation during crystal growth [28, 29]. For a given supersaturation, the radii of the hollow cores (if nonzero) are expected to increase with the strain energy of the dislocations which is proportional to the square of the Burgers vector, $\boldsymbol{b}^2$. Although, unfortunately, the supersaturation at which the final surface morphology was formed is not well known because of a shut-off effect, it can be assumed that dislocation outcrops in a small region of a growing face are exposed to the same supersaturation. In Fig. 2, as mentioned in Section 3.1.1, the radii of the hollow cores increase with the number of spiral layers that are connected with the hollow cores. Of the two dislocations capable to form single spiral centres, namely [1 0 0] and $[\bar{1}\ 1\ 1]$, the first one has a three times lower strain energy. From this, and the fact that the single spirals show the smallest hollow cores, it follows that the dislocations with $\boldsymbol{b} = [1\ 0\ 0]$ are more likely to be sources of the single spiral steps than those with $\boldsymbol{b} = [\bar{1}\ 1\ 1]$.

The dislocations with $\boldsymbol{b} = [1\ 0\ 0]$ were rarely found in the X-ray topographic study [9] and the corresponding single spiral hillocks were not found in the previous in situ investigation in a flowing solution [14]. Onuma et al. [18] showed that buoyancy driven convection plays a significant role in the formation of hoppered morphology and liquid inclusions. As mentioned in Section 3.1.1, such inclusions are obviously responsible for the high density of the dislocations in the crystal in the present experiment. From the above, it is suggested here that the dislocations with $\boldsymbol{b} = [1\ 0\ 0]$ are formed due to lattice enclosure errors after formation of liquid inclusions.

On the other hand, for the (1 0 0) faces, the dislocations that are capable to be spiral step sources are those with $\boldsymbol{b} = [1\ 0\ 0]$, $[1\ 1\ 0]$ and $[1\ 1\ 1]$. Of all these dislocations the component of the Burgers vector normal to the (1 0 0) growth face is $d_{1\ 0\ 0}$ (i.e. two growth layers $d_{2\ 0\ 0}$). On the (1 0 0) faces, therefore, only the spiral hillocks composed of double elementary layers as shown in Fig. 3 are created, regardless of the dislocation source.

4.2. Step splitting and activity of spiral hillocks

Step splitting was typically observed for multilayered spiral steps on $\{1\ 1\ 1\}$ faces. De Yoreo et al. [4] reported the same phenomenon on $\{1\ 0\ 1\}$ faces of KDP crystals grown in aqueous solutions. The free enthalpy of step edges is expressed as $G = H - TS$, with H being the step enthalpy (which is very close to the step energy), T the growth temperature and S the entropy of the step. Assuming that step overhang does not occur at bunched steps, and assuming a relatively small step separation, the entropy term associated with the kink density increases with the separation between adjacent steps. As a consequence, the free enthalpy decreases for increasing step separation and very close steps are not favourable from a thermodynamic point of view [30]. This was confirmed by a recent Monte Carlo simulation of a sequence of steps on the $\{0\ 0\ 1\}$ surface of a Kossel crystal in the presence of surface diffusion [31]. At the centre of a spiral consisting of two or three layers the steps are very close to each other and tend to repel each other due to entropy repulsion. This explains the splitting of steps right from the beginning, when they are 'formed' at the spiral centres.

The splitting of spiral steps as described above can explain the difference in growth rate of individual spiral hillocks as reported in Ref. [14]. Provided that m-layered spiral steps decompose into elementary steps at the spiral centres, the interstep distance of an m-layered spiral will be $1/m$ times that of a single spiral on the average. From this it follows that the slope p of the former would be m times as large as that of the latter. From this, and the fact that the growth rate R of spiral hillocks, in the absence of interacting diffusion fields around adjacent steps, is given by $R = pv$ with v being the step velocity, the growth rate of m-layered spiral hillocks should be m times larger than that of a single-spiral hillock. In other words, the higher the total step height at the spiral centres, the larger the growth rate. On the $\{1\ 1\ 1\}$ faces of $Ba(NO_3)_2$,

therefore, the triple spiral centres are expected to be the strongest, the double ones are second and the single ones must be the weakest. This is partly confirmed by the results reported in a flowing solution [14], where the triple spiral centres showed steeper slopes and larger growth rates than the double ones. On the other hand, on the {1 0 0} faces, such a variation in the growth rate of spiral centres due to a difference in the total step height is not expected, because only double layered steps are formed by dislocations on these faces as mentioned in Section 4.1.

5. Conclusions

AFM is a very powerful method for the ex situ examination of step patterns on the surfaces of crystals grown from solution. By this technique growth steps of monomolecular height on the {1 0 0} and the {1 1 1} faces of $Ba(NO_3)_2$ crystals grown from aqueous solutions have been imaged and analysed. From these investigations, amongst others, the following can be concluded:

1. Spiral growth and 2D nucleation growth were observed on both the {1 1 1} and the {1 0 0} faces. It was confirmed that the growth proceeds via the elementary steps that are expected from BFDH and PBC theory: $d_{1\,1\,1}$ and $d_{2\,0\,0}$ on the {1 1 1} and the {1 0 0} faces, respectively.
2. 2D nuclei observed in this study were probably formed during a period of very high supersaturation when the crystals were removed from the solution.
3. Single and multiple spiral layers arise from dislocation outcrops on the growing faces. Depending on the Burgers vectors of the central dislocation, spirals composed of single, double and triple layers on the {1 1 1} faces and double layers on the {1 0 0} faces are formed. The multiple steps tend to split into elementary steps, probably due to entropic repulsion.
4. Hollow cores, with radii of 7–15 nm on {1 1 1} and 30–50 nm on {1 0 0}, were observed at dislocation outcrops. These radii of hollow cores increase with the number of spiral steps associated with the dislocations.

Acknowledgements

The authors would like to thank Dr. H. Meekes and Drs. R.F.P. Grimbergen, University of Nijmegen, for valuable discussions. Two of the authors (K.M. and M.P.) acknowledge financial support from the Science and Technology Agency, Japan and the Dutch Organization for Chemical Research (SON), respectively.

References

[1] For example, Yu. G. Kuznetsov, A.J. Malkin, W. Glantz, A. McPherson, J. Crystal Growth 168 (1996) 63, and references therein.
[2] A.J. Gratz, P.E. Hillner, P.K. Hansma, Geochim. Cosmochim. Acta 57 (1993) 491.
[3] A.J. Gratz, S. Manne, P.K. Hansma, Science 251 (1991) 1343.
[4] J.J. De Yoreo, T.A. Land, B. Dair, Phys. Rev. Lett. 73 (1994) 838.
[5] K. Tsukamoto, H. Ohba, I. Sunagawa, J. Crystal Growth 63 (1983) 18.
[6] M. Ribet, J.L. Ribet, F. Lefaucheux, M.C. Robert, J. Crystal Growth 49 (1980) 334.
[7] M.C. Robert, F. Lefaucheux, M. Sauvage, M. Ribet, J. Crystal Growth 52 (1981) 976.
[8] M. Ribet, A. Authier, J. Crystal Growth 57 (1982) 541.
[9] K. Maiwa, K. Tsukamoto, I. Sunagawa, J. Crystal Growth 82 (1987) 611.
[10] B.Yu. Shekunov, L.N. Rashkovich, I.L. Smol'skii, J. Crystal Growth 116 (1992) 340.
[11] K. Maiwa, K. Tsukamoto, I. Sunagawa, C.-z. Ge, N.-b. Ming, J. Crystal Growth 98 (1989) 590.
[12] C.-z. Ge, N.-b. Ming, K. Tsukamoto, K. Maiwa, I. Sunagawa, J. Appl. Phys. 69 (1991) 7556.
[13] L.N. Rashkovich, B.Yu. Shekunov, V.N. Voitsekhovskii, M.V. Shvedova, Sov. Phys. Crystallogr. 34 (1989) 925.
[14] K. Maiwa, K. Tsukamoto, I. Sunagawa, J. Crystal Growth 102 (1990) 43.
[15] I. Sunagawa, K. Tsukamoto, K. Maiwa, K. Onuma, Prog. Crystal Growth Charact. 30 (1995) 153.
[16] K. Onuma, T. Kameyama, K. Tsukamoto, J. Crystal Growth 137 (1994) 610.
[17] K. Onuma, K. Tsukamoto, I. Sunagawa, J. Crystal Growth 89 (1988) 177.
[18] K. Onuma, K. Tsukamoto, I. Sunagawa, J. Crystal Growth 98 (1989) 384.
[19] W.J.P. van Enckevort, Current Topics Crystal Growth Res. 2 (1995) 535.
[20] L. Vegard, Z. Phys. 9 (1922) 395.
[21] F.M. Jäger, F.A. van Melle, Proc. K. Ned. Akad. Wet. 31 (1928) 651.
[22] W.C. Hamilton, Acta Crystallogr. 10 (1957) 103.
[23] G. Lutz, Z. Kristallogr. 114 (1960) 232.

[24] H. Nowotny, G. Heger, Acta Crystallogr. C 39 (1983) 952.
[25] R. Birnstock, Z. Kristallogr. 124 (1967) 310.
[26] M. Plomp, K. Maiwa, W.J.P. van Enckevort, P. Bennema, to be published.
[27] See, P. Bennema, in: D.T.J. Hurle (Ed.), Handbook of Crystal Growth, 1a. Thermodynamics and Kinetics, North-Holland, Amsterdam, 1993, p. 477.
[28] F.C. Frank, Acta Crystallogr. 4 (1951) 497.
[29] B. Van der Hoek, J.P. Van der Eerden, P. Bennema, J. Crystal Growth 56 (1982) 621.
[30] X.-S. Wang, J.L. Goldberg, N.C. Bartelt, T.L. Einstein, E.D. Williams, Phys. Rev. Lett. 65 (1990) 2430.
[31] N.C. Bartelt, T.L. Einstein, E.D. Williams, Surf. Sci. 312 (1994) 411.